Electronic Supplementary Material (ESI) for Analyst.

Isothermal Strand Displacement Amplification (iSDA): A Rapid and Sensitive Method of Nucleic Acid Amplification for Point-of-Care Diagnosis

Bhushan J. Toley*, Isabela Covelli, Yevgeniy Belousov†, Sujatha Ramachandran, Enos Kline, Noah Scarr†, Nic Vermeulen†, Walt Mahoney†, Barry R. Lutz, Paul Yager

Department of Bioengineering
University of Washington
Seattle, WA 98195-5061

† ELITechGroup Inc. Molecular Diagnostics
Bothell, WA 98021

Running Title: Isothermal strand displacement amplification (iSDA)

Keywords: Lateral flow assay, nicking enzyme, primer asymmetry, primer dimers, kinetic modeling, low resource settings

Table of Contents

*Correspondence to:
Bhushan J. Toley
Department of Bioengineering
University of Washington
Box 355061, Foege N107
3720 15th Ave NE
Seattle, WA 98195-5061
Phone: 206-543-8063
Email: btoley@uw.edu

SUPPORTING INFORMATION

S1: Primer and Probe Sequences

For the *ldh1* iSDA assay, extension primers (E1, E2) and bumper primers (B1, B2) had the following sequences (the underlined sequence shows the nicking site):

E1: GCATAATACTACCAGTCTCCTCAGCAAGCTACGCATTTTCATTAG

E2: TAGAATAGTCGCATACTTCCTCAGCCATAACATCTCCTCGAACT

B1: AGGTAATGGTGCAGTAGGT

B2: CCAGCTTTCACACGAAC

Probe sequences are provided below. Biotin was conjugated to probes using a triethyleneglycol (TEG) linker.

Capture probe: [TTTTTTTTC]-(Q14)- CAGTGTCTAAATCAATGATG, where the sequence within square brackets is composed of pDNA.

Biotin probe: CTAATTCATCAACAATGC-biotin TEG

The fluorescent Pleiades probe had the same sequence as biotin probe and used a FAM fluorophore.

For the IC iSDA assay, extension primers ($E1_{IC}$, $E2_{IC}$) and bumper primers ($B1_{IC}$, $B2_{IC}$) had the following sequences:

$E1_{IC}$: CCAATATAGTAACAGTCTCCTCAGCATTCGCCCTTCTGCACG

$E2_{IC}$: TTCAAAAGACCCATACTTCCTCAGCCTTCTCATTTTTTCTACCG

$B1_{IC}$: TCGGATCCACTAGTAAC

$B2_{IC}$: GTGATGGATATCTGCAGAAT

The following probes were used:

Capture probe: [ACATCACA]-Q14-GATCTTGTACCAATGC

Biotin probe: CGTGGTCCGTAAAG-biotin TEG

The fluorescent Pleiades probe had the same sequence as biotin probe and used an AquaFluor® 525 (AP525; A Trademark of ElitechGroup S.A.S.) fluorophore.

S2: Calculation of Normalized Integrated Line Intensities (I_{test}) from Lateral Flow Strips

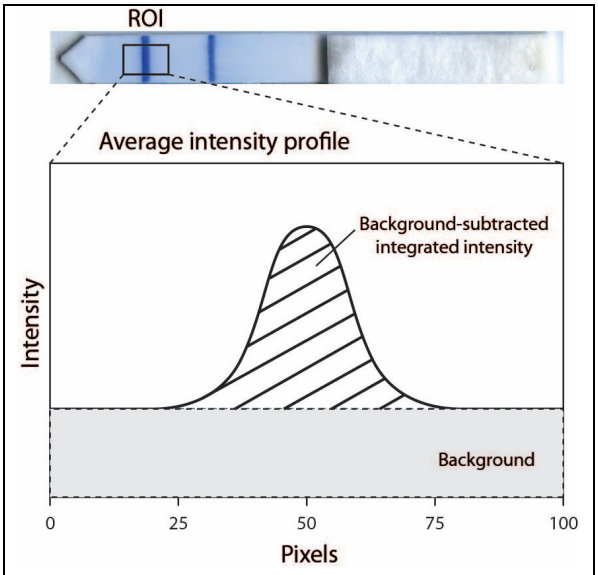

Figure S-1. Calculation of background-subtracted integrated line intensities.

The colored image obtained from the scanner was split into three color channels using ImageJ (NIH Research Services) and the red channel was chosen for analysis. A rectangular region of interest (ROI), 100 pixels length x 65 pixels width, was drawn over the test line such that the length of the ROI was in the direction of flow (Fig. S-1). An average linear intensity profile was created by averaging intensities across successive widths of the ROI. A background-subtracted integrated intensity was obtained by calculating the area under this curve and subtracting the area under the background intensity value, as demonstrated in Figure S1. Area under the curve was calculated using the trapezoidal rule using Excel (Microsoft, Redmond, WA). The dashed area of the graph indicates the area that is reported as the integrated signal line intensity. Finally, each set of data were normalized by the maximum integrated intensity in that set to obtain values in the range of 0 to 1.

S3: Polyacrylamide Gel Electrophoresis (PAGE)

PAGE analysis was conducted under denaturing conditions. A 2.2 µl sample (from a 10 µl reaction) was mixed with 3.3 µl gel loading buffer II (Life Technologies, Carlsbad, CA) and 1.1 µl of molecular grade water (Corning, Manassas, VA), heated to 95°C for 5 minutes, then kept on ice. 6 µl of this sample mix was loaded into pre-cast 15% Novex® TBE-Urea gels (Life Technologies). A 10bp ladder (Life Technologies) was used as a marker. Electrophoresis was conducted in an XCell SureLock™ Mini-Cell Electrophoresis System (Life Technologies) at 160 volts for ~40 minutes using a 1x TBE running buffer. The electrophoresis cell was kept in a pre-warmed water bath at 70°C to ensure that denaturing conditions were maintained throughout. After electrophoresis, gels were stained with 2x SYBR Gold® Nucleic Acid Gel Stain (Life Technologies) in 1x TBE for 20 minutes. Stained gels were imaged using a Gel Doc™ EZ System (Bio-Rad, Hercules, CA).

S4: A Simple Mathematical Model of iSDA

S4.1 List of Reactions

The following list of reactions was derived from the reaction networks shown in Figure S2:

Target Amplification Pathway (Fig. 4A)

(1) Nicking

$$D' + E_N \underset{k_{offN}}{\overset{k_{onN}}{\leftrightarrow}} DA'.E_N \xrightarrow{k_{catN}} E_N + DAN'$$

$$D' + E_N \underset{k_{offN}}{\overset{k_{onN}}{\leftrightarrow}} DB'.E_N \xrightarrow{k_{catN}} E_N + DBN'$$

(2) Extension (with strand displacement)

$$DAN' + E_P \underset{k_{offP}}{\overset{k_{onP}}{\leftrightarrow}} DAN'.E_P$$

$$DAN'.E_P + dNTP \underset{k_{offdNTP}}{\overset{k_{ondNTP}}{\leftrightarrow}} DAN'.E_P.dNTP. \xrightarrow{k_{catP}} E_P + SA + D'$$

$$DBN' + E_P \underset{k_{offP}}{\overset{k_{onP}}{\leftrightarrow}} DBN'.E_P$$

$$DBN'.E_P + dNTP \underset{k_{offdNTP}}{\overset{k_{ondNTP}}{\leftrightarrow}} DBN'.E_P.dNTP. \xrightarrow{k_{catP}} E_P + SB + D'$$

(3) Primer and probe annealing

$$SA + E1 \underset{k_{offPri}}{\overset{k_{onPri}}{\leftrightarrow}} SA\text{-}E1$$

$$SA\text{-}E1 + F \underset{k_{offF}}{\overset{k_{onF}}{\leftrightarrow}} SA\text{-}F\text{-}E1$$

$$SA + F \underset{k_{offF}}{\overset{k_{onF}}{\leftrightarrow}} SA\text{-}F$$

$$SA\text{-}F + E1 \underset{k_{offPri}}{\overset{k_{onPri}}{\leftrightarrow}} SA.F.E1$$

$$SB + E2 \underset{k_{offPri}}{\overset{k_{onPri}}{\leftrightarrow}} SB\text{-}E2$$

(4) Extension (without strand displacement)

$$SA\text{-}E1 + E_P \underset{k_{offP}}{\overset{k_{onP}}{\leftrightarrow}} SA\text{-}E1.E_P$$

$$SA\text{-}E1.E_P + dNTP \underset{k_{offdNTP}}{\overset{k_{ondNTP}}{\leftrightarrow}} SA\text{-}E1.E_P.dNTP \xrightarrow{k_{catP}} E_P + D'$$

$$SA\text{-}F\text{-}E1 + E_P \underset{k_{offP}}{\overset{k_{onP}}{\leftrightarrow}} SA\text{-}F\text{-}E1.E_P$$

$$SA\text{-}F\text{-}E1.E_P + dNTP \underset{k_{offdNTP}}{\overset{k_{ondNTP}}{\leftrightarrow}} SA\text{-}F\text{-}E1.E_P.E_P.dNTP \xrightarrow{k_{catP}} E_P + D' + F$$

$$SB\text{-}E2 + E_P \underset{k_{offP}}{\overset{k_{onP}}{\leftrightarrow}} SB\text{-}E2.E_P$$

$$SB\text{-}E2.E_P + dNTP \underset{k_{offdNTP}}{\overset{k_{ondNTP}}{\leftrightarrow}} SB\text{-}E2.E_P.dNTP \xrightarrow{k_{catP}} E_P + D'$$

(5) Annealing of complementary amplicons

$$SA + SB \underset{k_{offSS}}{\overset{k_{onSS}}{\leftrightarrow}} SA\text{-}SB$$

Primer-Dimer Amplification Pathway (Fig. 4B)

(1) Primer-dimer formation and extension

$$\text{E1+E2} \underset{k_{offPD}}{\overset{k_{onPD}}{\leftrightarrow}} \text{E1-E2}$$

$$\text{E1-E2} + \text{E}_\text{P} \underset{k_{offP}}{\overset{k_{onP}}{\leftrightarrow}} \text{E1-E2.E}_\text{P}$$

$$\text{E1-E2.E}_\text{P}\text{+dNTP} \underset{k_{offdNTP}}{\overset{k_{ondNTP}}{\leftrightarrow}} \text{E1-E2.E}_\text{P}\text{.dNTP} \xrightarrow{k_{catP}} \text{E}_\text{P}\text{+P}$$

(2) Nicking of primer-dimer complex

$$\text{P+E}_\text{N} \underset{k_{offN}}{\overset{k_{onN}}{\leftrightarrow}} \text{PA}'\text{.E}_\text{N} \xrightarrow{k_{catN}} \text{E}_\text{N}\text{+PAN}$$

$$\text{P+E}_\text{N} \underset{k_{offN}}{\overset{k_{onN}}{\leftrightarrow}} \text{PB}'\text{.E}_\text{N} \xrightarrow{k_{catN}} \text{E}_\text{N}\text{+PBN}$$

(3) Extension with strand displacement from primer-dimer complex

$$\text{PAN+E}_\text{P} \underset{k_{offP}}{\overset{k_{onP}}{\leftrightarrow}} \text{PAN.E}_\text{P}$$

$$\text{PAN.E}_\text{P}\text{+dNTP} \underset{k_{offdNTP}}{\overset{k_{ondNTP}}{\leftrightarrow}} \text{PAN.E}_\text{P}\text{.dNTP.} \xrightarrow{k_{catP}} \text{E}_\text{P}\text{+SPA+P}$$

$$\text{PBN+E}_\text{P} \underset{k_{offP}}{\overset{k_{onP}}{\leftrightarrow}} \text{PBN. E}_\text{P}$$

$$\text{PBN.E}_\text{P}\text{+dNTP} \underset{k_{offdNTP}}{\overset{k_{ondNTP}}{\leftrightarrow}} \text{PBN.E}_\text{P}\text{.dNTP.} \xrightarrow{k_{catP}} \text{E}_\text{P}\text{+SPB+P}$$

(4) Primer annealing

$$\text{SPA+ E2} \underset{k_{offPri}}{\overset{k_{onPri}}{\leftrightarrow}} \text{SPA-E2}$$

$$\text{SPB+ E1} \underset{k_{offPri}}{\overset{k_{onPri}}{\leftrightarrow}} \text{SPB-E1}$$

(5) Extension (without strand displacement)

$$\text{SPA-E2+E}_\text{P} \underset{k_{offP}}{\overset{k_{onP}}{\leftrightarrow}} \text{SPA-E2.E}_\text{P}$$

$$\text{SPA-E2.E}_\text{P}\text{+dNTP} \underset{k_{offdNTP}}{\overset{k_{ondNTP}}{\leftrightarrow}} \text{SPA-E2.E}_\text{P}\text{.dNTP} \xrightarrow{k_{catP}} \text{E}_\text{P}\text{+P}$$

$$\text{SPB-E1+E}_\text{P} \underset{k_{offP}}{\overset{k_{onP}}{\leftrightarrow}} \text{SPB-E1.E}_\text{P}$$

$$\text{SPB-E1.E}_\text{P}\text{+dNTP} \underset{k_{offdNTP}}{\overset{k_{ondNTP}}{\leftrightarrow}} \text{SPB-E1.E}_\text{P}\text{.dNTP} \xrightarrow{k_{catP}} \text{E}_\text{P}\text{+P}$$

(6) Annealing of complementary amplicons

$$\text{SPA+ SPB} \underset{k_{offPri}}{\overset{k_{onPri}}{\leftrightarrow}} \text{SPA-SPB}$$

In the above reaction scheme, E_N and E_P are nicking enzyme and polymerase, respectively. For the sake of simplicity, the four nucleotides were denoted by a single species, dNTP, composed of

112 nucleotides, the mean size of the two target amplicons. Primer dimer amplicons are shorter than target amplicons, but in this model, for simplicity, they are also assumed to consume 112-mer nucleotides. Enzyme complexes are denoted by a '.' symbol, for example DAN'.E_P is a complex of DAN' and E_P. The forward and reverse rate constants of SPA and SPB binding to produce SPA-SPB are assumed to be equal to those of primer binding to target, because SPA and SPB are not significantly longer strands than the primers.

S4.2 Model Parameters

Table S-1 shows the parameter values used to solve the model. All parameter values were obtained from literature, except k_{S2} and k_{-S2}, the rates of primer dimer formation and dissociation, respectively, which were adjusted to reflect experimentally observed data.

Table S-1: Model parameter values

Parameter	Description	Value	Source
k_{onN}	Rate of nicking enzyme associating to substrate	0.1 $nM^{-1}s^{-1}$	Bellamy et al.
k_{offN}	Rate of nicking enzyme dissociating from substrate	10 s^{-1}	Mehra et al.
k_{catN}	Catalytic rate of nicking enzyme	0.17 s^{-1}	Bellamy et al
k_{onP}	Rate of polymerase associating to substrate	0.1 $nM^{-1}s^{-1}$	Mehra et al.
k_{offP}	Rate of polymerase dissociating from substrate	10 s^{-1}	Mehra et al.
k_{catP}	Catalytic rate of polymerase	0.283 s^{-1}	Montagne et al.
k_{ondNTP}	Rate of dNTP association	5e-4 $nM^{-1}s^{-1}$	Mehra et al.
$k_{offdNTP}$	Rate of dNTP dissociation	1e-4 s^{-1}	Mehra et al.
k_{onPri}	Rate of primer annealing to target	5e-4 $nM^{-1}s^{-1}$	Mehra et al.
k_{offPri}	Rate of primer dissociation from target	1e-4 s^{-1}	Mehra et al.
k_{onF}	Rate of fluorescent probe annealing to target	1e-4 $nM^{-1}s^{-1}$	Lukhtanov et al.
k_{offF}	Rate of fluorescent probe dissociation from target	1e-4 s^{-1}	Mehra et al.
k_{onSS}	Rate of binding of sense and antisense amplicons	5e-4 $nM^{-1}s^{-1}$	N/A
k_{offSS}	Rate of dissociation of sense and antisense amplicons	1e-4 s^{-1}	N/A
k_{onPD}*	Rate of association of primer-dimers	1e-7 $nM^{-1}s^{-1}$	N/A
k_{offPD}	Rate of dissociation of primer-dimers	2e7 s^{-1}	N/A

*The parameter k_{onPD} was set to zero for generating the curves shown in Fig. 4F.

S4.3 Initial Values

Initial concentration values used for solving the model were determined by concentrations of starting species in experiments and are shown in Table S-2. Experiments used 200 μM each of four nucleotides. The species, dNTP, used in the model is assumed to be a 112-mer of individual nucletides. Thus the initial concentration of dNTP was calculated as follows:

$$\mathrm{dNTP} = \frac{4 \times 200\mu\mathrm{M} \times 1000 \frac{\mathrm{nM}}{\mu\mathrm{M}}}{112 \text{ nucleotides}} = 7142 \text{ nM}$$

Initial concentrations of extension primers E1 and E2, and fluorescent probe, F, was set to those used in experiments (Table S-2). For species D', the number of input copies in a 10 μl reaction was converted into a concentration expressed in units of nM, e.g. for 100 input copies, initial concentration was calculated as follows:

$$D' = \frac{100 copies}{6\text{x}10^{23} \frac{copies}{mole} \text{x} \frac{1 mole}{10^9 nmoles} \text{ x } 10\mu l \text{ x} \frac{1 l}{10^6 \mu l}} = 1.67\text{x}10^{-8} nM$$

In this embodiment of the model, the starting enzyme concentrations were selected by trial and error to match model output to experimental data.

Table S-2: Initial values

Species	Initial Concentration (nM)
D'	$1.67\text{x}10^{-8}$ (for 100 copies and scaled accordingly)
E_N	100
E_P	250
dNTP	7142
E1	250
E2	500
F	200

S4.4 Model Validation

Additional model validation is presented here. The model successfully predicted the experimentally observed effects of contamination of iSDA reactions with amplified off-target products, or products of NTC reactions, represented in the model by the sum of concentrations of species P, PAN, PBN, SPA, SPB, SPA-E2, SPB-E1, and SPA-SPB (Fig. S-2). Experimentally, it was observed that the amplification of 1000 *ldh1* copies by iSDA was inhibited when reactions were contaminated with products of NTC reactions conducted previously. This is a result of competition between *ldh1* amplification and amplification of template-independent side products.

Experiment: First, a set of NTC iSDA reactions was conducted. Products of these NTC reactions were serially diluted 10x in water to a maximum dilution of 10^{14}x. A 1-µl solution of these diluted NTC products was introduced in iSDA reactions containing 1000 *ldh1* copies. Average of three experimentally obtained *ldh1* amplification curves are shown in Fig. S-3A. The positive control condition (red curve; Fig. S-3A) was not contaminated with NTC products, and green, blue, and black curves (Fig. S-3A) represent reactions contaminated with 10^{14}x, 10^{8}x, and 10^{4}x-diluted NTC products. 10^{14}x-diluted NTC products did not have a negative effect on *ldh1* amplification compared to the positive control (green and red curves; Fig. S-3A). 10^{8}x-diluted NTC products reduced the average plateau level of the curves (blue curve; Fig. S-3A) and 10^{4}x-diluted NTC products completely eliminated detectable product from the *ldh1* iSDA reaction (black curve; Fig. S-3A).

Model: These conditions were replicated in the mathematical model. First, the model was solved for the NTC condition, i.e. for 0 *ldh1* copies. The concentrations of species P, PAN, PBN, SPA, SPB, SPA-E2, SPB-E1, and SPA-SPB predicted by the model were noted. The model was then solved for 1000 *ldh1* copies, but the initial concentrations of all primer-dimer amplification species noted above were set to reflect the amount of diluted NTC product introduced in the experiments. Amplification curves predicted by the model are shown in Fig. S-3B. The model, qualitatively, predicts the behavior of experiments (Fig. S-3A). The red and green curves for positive control (no contamination) and reactions contaminated with 10^{14}x-diluted NTC products, respectively, overlap, implying that there was no deleterious effect at this concentration of NTC product. At 10^{8}x-dilution, the plateau level of the curve decreased (blue curve; Fig. S-3B) and 10^{4}x-dilution, the production of *ldh1* amplicons was completely inhibited (black curve; Fig. S-3B). These results qualitatively match experiments (Fig. S-3A) very well.

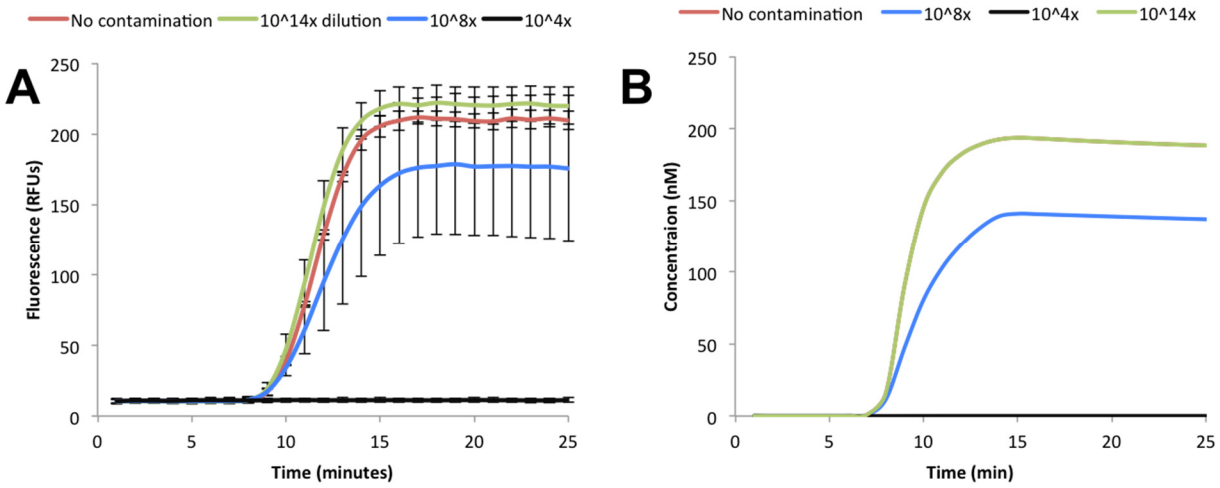

Figure S-3. Contamination of iSDA reactions by products of NTC iSDA reactions. Comparison of experimental (A) and model results (B). All reactions contained 1000 *ldh1* copies. Positive controls were not contaminated with NTC products (red curves) and other conditions represent contamination of iSDA reactions with different dilutions of NTC products.

S5: Fluorescence to Concentration Calibration

Fluorescence data obtained from the Rotorgene was converted into concentrations by conducting a fluorescence-concentration calibration using synthetic truncated amplicons. Synthetic truncated amplicons contained probe-binding regions, but not regions complementary to primers. When added to an iSDA reaction, they can be detected by probes, but cannot amplify because they lack primer-binding regions. Different concentrations of the synthetic amplicons were added to mock iSDA reactions that did not contain *ldh1* template DNA, but contained all other reaction components. The reactions were incubated at 49°C for 30 minutes, similar to regular iSDA reactions, and fluorescence readings were obtained at 30 minutes. Fig. S-4A shows the obtained calibration curve. The concentration of fluorescent Pleiades probe used was 200 nM, equal to that used in iSDA reactions. As a result, the curve plateaued for concentrations of synthetic amplicons greater than 200 nM. The linear portion of the calibration curve was in between 0 to 200 nM (Fig. S-4B) and fit a straight line well ($R^2 = 0.9956$).

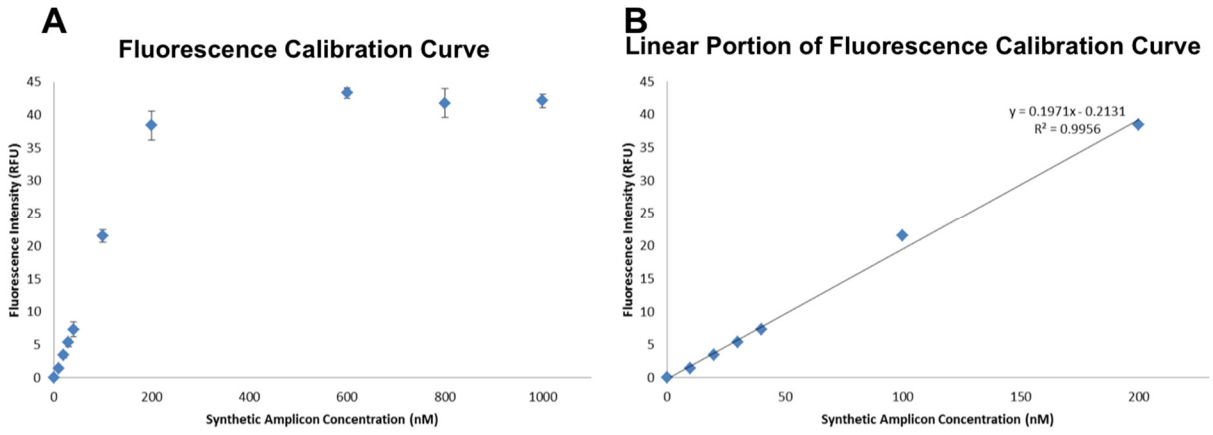

Figure S-4. Fluorescence-concentration calibration curve. **A**. Calibration curve over the entire range of synthetic amplicon concentration. **B**. Linear portion of the calibration curve. 3 replicates were obtained at each concentration. Error bars represent standard deviation.

References

- Bellamy, S. R. *et al.* Cleavage of individual DNA strands by the different subunits of the heterodimeric restriction endonuclease BbvCI. *J Mol Biol* **348**, 641-653, doi:10.1016/j.jmb.2005.02.035 (2005).
- Mehra, S. & Hu, W. S. A kinetic model of quantitative real-time polymerase chain reaction. *Biotechnol Bioeng* **91**, 848-860, doi:10.1002/bit.20555 (2005).
- Montagne, K., Plasson, R., Sakai, Y., Fujii, T. & Rondelez, Y. Programming an in vitro DNA oscillator using a molecular networking strategy. *Mol Syst Biol* **7**, 466, doi:10.1038/msb.2010.120 (2011).
- Lukhtanov, E. A., Lokhov, S. G., Gorn, V. V., Podyminogin, M. A. & Mahoney, W. Novel DNA probes with low background and high hybridization-triggered fluorescence. *Nucleic Acids Res* **35**, e30, doi:10.1093/nar/gkl1136 (2007).